Electronic Supplementary information

A novel bio-template route to synthesize enzyme-immobilized MOF/LDHs tubular magnetic micromotors and their application in water treatment

Xiaohan Yang, Chenzhang Liu, Shuo Gao, Xiaolei Zhang, Ziwei Lan, Min Zuo, Jia Li[1]

School of Material Science and Engineering, University of Jinan, Jinan, China

1. Figures

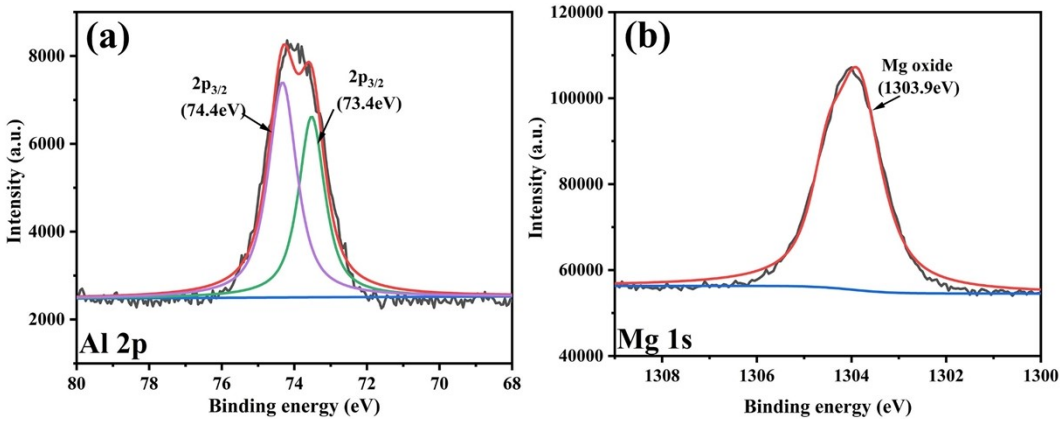

Fig. S1 XPS spectra of Al 2p (a), Mg 1s (b).

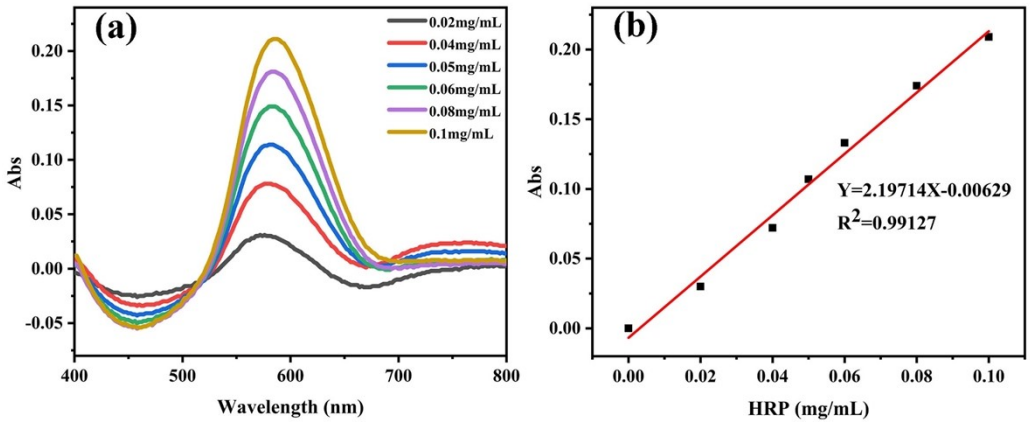

Fig. S2 UV-Vis absorption spectra of HRP enzyme tested by the Kaumas Brilliant Blue method (a) and its standard curve (b).

[1] Corresponding author. E-mail: mse_lij@ujn.edu.cn (J. Li).

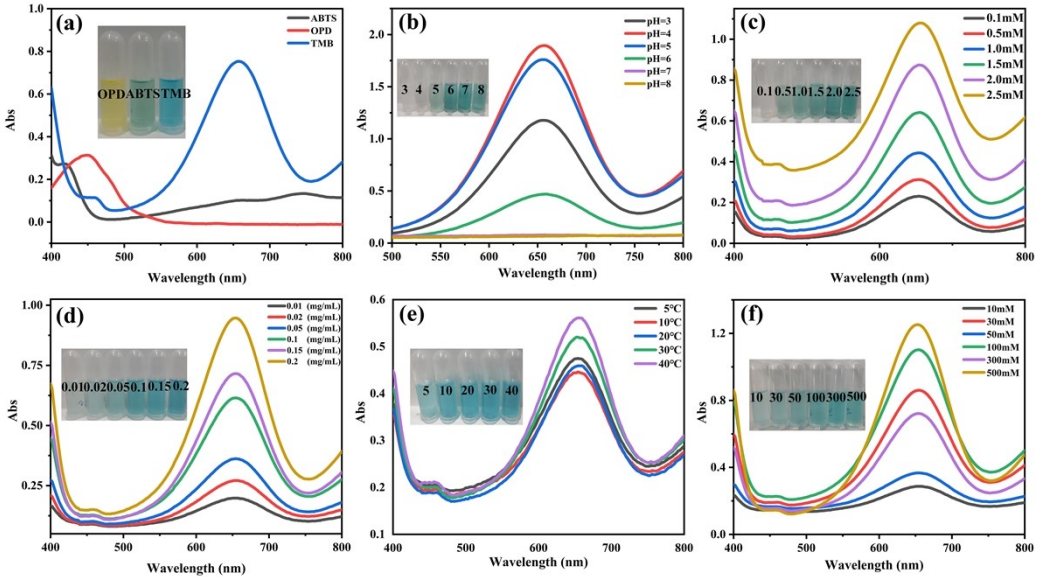

Fig. S3 Effect of different chromogenic substrates, time (a), pH (b), catalyst concentration (c), TMB concentration (d), temperature (e) and H_2O_2 concentration (f) on the chromogenic reaction system.

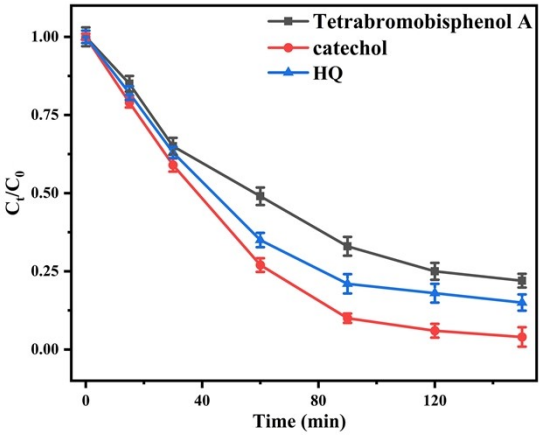

Fig. S4 Degradation rates of catechol, hydroquinone, and tetrabromobisphenol A under the same conditions.

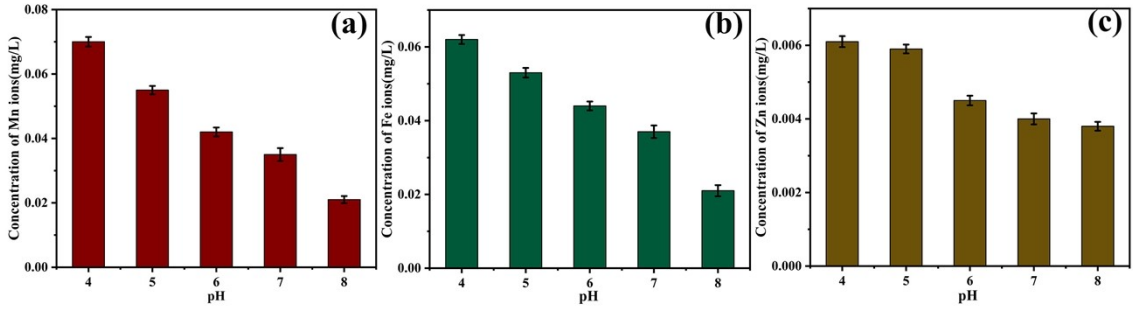

Fig. S5 Manganese ion leaching during degradation (a), iron ion leaching (b), zinc ion leaching (c).

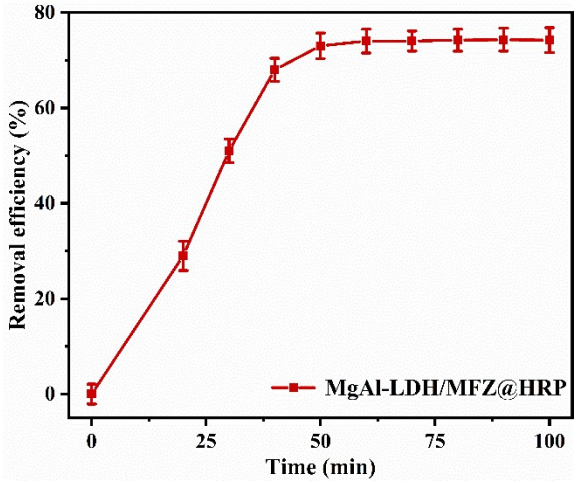

Fig. S6 Effect of adding MgAl-LDH/MFZ@HRP micromotor on COD removal efficiency of catechol practical wastewater.

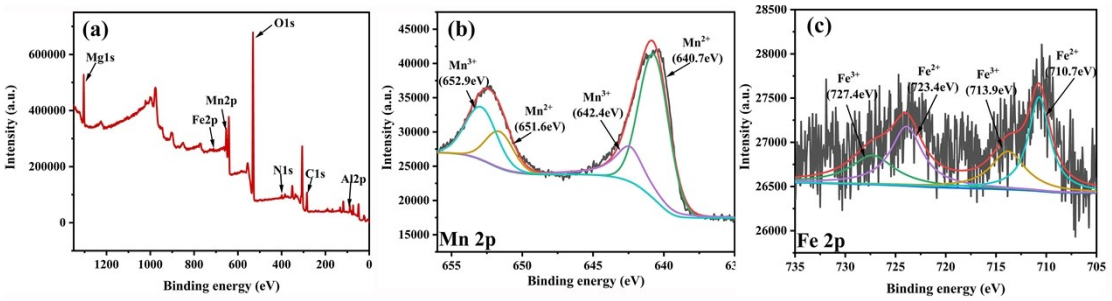

Fig. S7 XPS plots of degraded MgAl-LDH/MFZ@HRP micromotors, full spectrum (a), Mn (b), Fe (c).

2. Table

Table S1 Pore texture parameters of the obtained samples

Sample	SBET (m^2 g^{-1})	VTotal (cm^3 g^{-1})	Dp (nm)
Mn_2O_3/C	44.929	0.160341	14.4125
MgAl-LDH	65.7686	0.157659	10.5368
MgAl-LDH/MFZ@HRP	110.6669	0.25114	8.6179

Table S2 Comparison of speed with other reported micromotors

Micromotors	Concentration of H_2O_2	Velocity (μm s^{-1})	Ref.
CuS@Fe_3O_4/Pt	5%	423.8	[1]
Magnetic illite microspheres	5%	100.38	[2]
MnO_2 microparticles	5%	128	[3]
Au/ Ni/Pt	5%	37.57	[4]
Fe-zeolite	10%	84.96	[5]
rGO/ZnO/BiOI/Co-Pi/Pt	5%	63.1	[6]
PAPBA/Ni/Pt	3%	40	[7]
MgAl-LDHs/MFZ	3%	128.33	This work

Table S3 Comparison of various sensor platforms for the detection of catechol

Method	System	LOD (μM)	Linear(μM)	Ref.
Electrochemical	AuNP-MoS_2-Lac/GCE	2.0	2-2000	[8]
Electrochemical	FYSSns-2-Lac/GCE	1.6	12.5-450	[9]
Electrochemical	Fe_3O_4-GO-AuNPs	0.8	2-145	[10]
Colorimetric	TMB-δ-MnO_2	0.22	0.5-10	[11]
Colorimetric	$Co_{1.5}Mn_{1.5}O_4$	0.35	1-1000	[12]
Colorimetric	MgAl-LDH/MFZ@HRP	0.69	0-200	This work

Table S4 Comparison of COD before and after degradation of actual catechol wastewater

Actual water sample status	Testing Program	Test results (mg/L)
pre-degradation	CODCr	192.23
after degradation		49.21

References

1. E. H. Ma, K. Wang, Z. Q. Hu and H. Wang, Dual-stimuli-responsive CuS-based micromotors for efficient photo-Fenton degradation of antibiotics, *J. Colloid Interface Sci.*, 2021, **603**, 685-694.
2. C. W. Park, T. Kim, H. M. Yang, Y. Lee and H. J. Kim, Active and selective

removal of Cs from contaminated water by self-propelled magnetic illite microspheres, *J. Hazard. Mater.*, 2021, **416**, 8.

3. J. Tesar, M. Ussia, O. Alduhaish and M. Pumera, Autonomous self-propelled MnO_2 micromotors for hormones removal and degradation, *Appl. Mater. Today*, 2022, **26**, 5.
4. Z. H. Li, Z. Z. Xie, H. Lu, Y. Wang and Y. S. Liu, Cargo Transportation and Methylene Blue Degradation by Using Fuel-Powered Micromotors, *ChemistryOpen*, 2021, **10**, 861-866.
5. W. Ma, K. Wang, S. H. Pan and H. Wang, Iron-Exchanged Zeolite Micromotors for Enhanced Degradation of Organic Pollutants, *Langmuir*, 2020, **36**, 6924-6929.
6. H. J. Zhou, B. Wu, L. Dekanovsky, S. Y. Wei, B. Khezri, T. Hartman, J. H. Li and Z. Sofer, Integration of BiOI nanosheets into bubble-propelled micromotors for efficient water purification, *FlatChem*, 2021, **30**, 6.
7. F. Kuralay, S. Sattayasamitsathit, W. Gao, A. Uygun, A. Katzenberg and J. Wang, Self-Propelled Carbohydrate-Sensitive Microtransporters with Built-In Boronic Acid Recognition for Isolating Sugars and Cells, *J. Am. Chem. Soc.*, 2012, **134**, 15217-15220.
8. Y. N. Zhang, X. Li, D. W. Li and Q. F. Wei, A laccase based biosensor on AuNPs-MoS_2 modified glassy carbon electrode for catechol detection, *Colloid Surf. B-Biointerfaces*, 2020, **186**, 7.
9. Y. J. Zheng, D. D. Wang, Z. K. Li, X. F. Sun, T. T. Gao and G. W. Zhou, Laccase biosensor fabricated on flower-shaped yolk-shell SiO_2 nanospheres for catechol detection, *Colloid Surf. A-Physicochem. Eng. Asp.*, 2018, **538**, 202-209.
10. S. Erogul, S. Z. Bas, M. Ozmen and S. Yildiz, A new electrochemical sensor based on Fe_3O_4 functionalized graphene oxide-gold nanoparticle composite film for simultaneous determination of catechol and hydroquinone, *Electrochim. Acta*, 2015, **186**, 302-313.
11. P. Y. Xiao, Y. Liu, W. J. Zong, J. Wang, M. H. Wu, J. J. Zhan, X. L. Yi, L. F. Liu and H. Zhou, Highly selective colorimetric determination of catechol based on the aggregation-induced oxidase-mimic activity decrease of δ-MnO_2, *RSC Adv.*, 2020,

10, 6801-6806.

12. X. X. Liu, J. Yang, J. Cheng, Y. Xu, W. Chen and Y. C. Li, Facile preparation of four-in-one nanozyme catalytic platform and the application in selective detection of catechol and hydroquinone, *Sens. Actuator B-Chem.*, 2021, **337**, 9.